Numerical Modelling of Microwave Heating Treatment for Tight Gas Sand Reservoirs

Hongcai Wang, Reza Rezaee, Ali Saeedi, Curtin University

Matthew Josh, CSIRO Earth Science and Resource Engineering, Perth, Australia

Abstract

Formation Heat Treatment (FHT) has been proved effective in removing water phase and creating micro-fractures in the near wellbore area previously. In order to improve the cost and time efficiency of FHT, microwave heater is considered as an alternative in this paper, and its feasibility in FHT is discussed in this paper. Numerical simulation is carried out to investigate the effects of microwave heating on reservoir quality and gas production. It is found that the water phase can be effectively removed by microwave heating, as a result, the relative permeability to gas increased significantly after heating. In terms of gas production rate, the cumulative gas in 90 days in heated well is 4×10^5 m^3 more than the non-heated well. As the most important parameter, the temperature distributions in the reservoir are computed with two methods and their value against the heating depth agree with each other reasonably. On the other hand, the surface temperature variations of three tight sandstone plugs are heated with microwave in the lab and their surface temperatures are carefully recorded against time. Then the laboratory data are compared with simulation results, and they correlate well with each other. The simulation work conducted in this paper shows the promising improvement of gas relative permeability and production by microwave heating.

Keywords: Tight gas reservoir; Formation Skin Damage; Microwave Heating; Numerical Modelling

1 Introduction

Water blocking is one of the major mechanisms of formation skin damage in tight gas reservoirs (Bahrami et al., 2011). It is a process related to the combined effects of adverse capillary pressure and relative permeability effects (Bennion, 2002). Figure 1 illustrates the evolution of the water trapping in a tight gas reservoir. The sub-irreducible water saturation, in which condition the initial water saturation is less than the irreducible water saturation, is the key reason to the establishment of phase trapping (Bennion, 1996). Once water invades in the formation, the water saturation increases dramatically and leads to a dramatic reduction of gas relative permeability. The formation will remain at higher water saturation than the initial water saturation. The reason for the difficulty of removing water phase in the near wellbore

area is the high capillary pressure of tight sandstone, which results from the extra small pore and pore throat size.

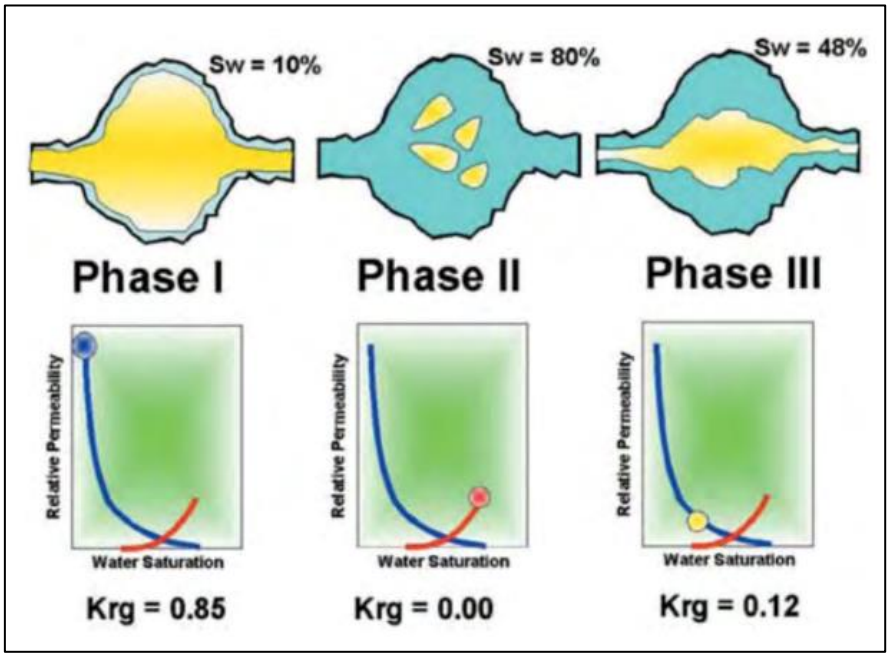

Figure 1 Illustration of Water Based Phase Trapping Effects in a Low Permeability Gas Reservoir (After Bennion, 2002).

Water blocking is one of the formation skin damages, which occurs in the near wellbore region with depth of invasion from several centimeters to about 2 meters. The depth of invasion (DI), which is defined as the distance from borehole wall, is a function of porosity and permeability. Miesch and Albright (1967) and Rider (2002) mentioned the relationship of porosity and the ratio of Depth of Invasion (DI) and Diameter of borehole (Table 1).

Table 1 Depth of Invasion Versus Porosity (After (Miesch & Albright, 1967) and (Rider, 2002)).

Hole size (in)	17.5	12.25	8.5	Ratio of Invasion Diameter to Hole Diameter
Porosity (%)	Depth of Invasion (cm)			
1-8	200.0	140.0	97.0	10
8-20	90.0	62.0	43.0	5
20-30	22.5	15.5	11.0	2
30+	3.0	2.0	1.7	<2

By regression study of experimental data, Yan, Jiang, and Wu (1997) revealed the empirical equation to calculate the invasion depth:

$$d = 1.612\Delta p^{0.521}\left(\frac{V_f}{\emptyset}\right)^{0.271} e^{0.043K}$$

Where d is the invasion depth (cm), Δp is the pressure differential in MPa, V_f is the cumulative filtrate loss in cm^3, $\emptyset$ is porosity (%), and K is permeability (μm^2).

The traditional Formation Heat Treatment (FHT) employs an electrical heater to raise the reservoir temperature and brings about the evaporation of blocked water, shrinkage of swollen clays and generation of micro-fractures, which enhances the reservoir quality of gas reservoirs. In this paper, microwave heating is considered as an alternative to traditional electrical heater because of its advantages in environmental friendliness, cost and time efficiency. The laboratory studies have indicated that the microwave heating can generate fractures in coal samples (Kumar, et al., 2011) and sandstone samples (Chen et al., 2015; Wang, et al., 2016). Note, this paper focuses on the effects of microwave heating on water saturation, relative permeability and finally the gas production rate. The influences of microwave heating on thermally induced fractures are not included in this paper.

Generally, microwave heating is a process of converting electromagnetic energy to heat. The dielectric properties of target material played the most vital role in this process. The propagation of electromagnetic wave was described by the following Maxwell's equations:

Gauss's law

$$\nabla \cdot \boldsymbol{E} = \frac{\rho}{\varepsilon_0}$$

Gauss's law for Magnetism

$$\nabla \cdot \boldsymbol{B} = 0$$

Maxwell-Faraday Equation

$$\nabla \times \boldsymbol{E} = -\frac{\partial B}{\partial t}$$

Ampere's Circuital Law

$$\nabla \times \boldsymbol{B} = \mu_0 (J + \varepsilon_0 \frac{\partial E}{\partial t})$$

Where, ∇ is the nabla symbol, $\nabla \cdot$ is divergence operator, $\nabla \times$ is a curl operator; $\boldsymbol{E}$ is the electric field; $\boldsymbol{B}$ is the magnetic field; ρ is the electric charge density; ε_0 is the permittivity of free space ($8.854\,187\,817 \times 10^{-12}$ F/m); μ_0 is the permeability of free space ($1.2566370614 \times 10^{-6}$ H/m); J is the current density.

Heat is generated in the reservoir by the interactions between microwave and molecular dipoles of reservoir rock and interstitial fluids. The dielectric properties of these materials, which relies on the mobility of the dipoles, determine the heating effects of microwave and tend to vary with temperature and frequency (Thostenson and Chou, 1999).

There are both bound charge and free charge in the dielectric materials. Polarization results from the motion of bound charge. Microwave heating is the consequence of dielectric relaxation due to polarization of electric charge or polarization of molecules (Thostenson and Chou, 1999).

The complex propagating factor of electromagnetic wave γ is given by (Metaxas and Meredith, 1983):

$$\gamma = \alpha + j\beta$$

Where, α is the attenuation factor and β is the phase factor. The wave is attenuated as it propagates in the media and the dissipated power reduces to some extent.

The rate of temperature rise is given by the following equation:

$$\frac{T - T_0}{t} = 0.556 \times \frac{10^{-10} \varepsilon_{eff}^{"} f E_{rms}^2}{\rho c_p} \ ^{\circ}\mathrm{C}\ s^{-1}$$

Where ε_{eff} is the effective dielectric loss, f is the electromagnetic wave frequency, E_{rms} is the electric field intensity, ρ is the material density (kg/m^3) and c_p is the specific heat (J/kg℃) (Metaxas and Meredith, 1983). For a fixed microwave source, for example, the frequency is 915 MHz or 2450 MHz, so the important parameters determining the temperature increase are the permittivity, density, specific heat and electric field, which is determined by the permittivity. In an actual reservoir, these vary with mineralogy, porosity, type of interstitial fluid and fluid saturation.

Microwave has a wide application in coal upgrading, cleaning and comminution. In terms of its application in sandstone, Li, et al. (2006) and Wang, et al. (2016) conducted laboratory studies on cleaning up water blocking in gas reservoirs using microwave heating. It is found that microwave heating can remove water saturation from the sample efficiently and may create fractures at the same time. Due to dehydration, the crystal structures of some minerals is changed after heating. Electromagnetic heating is also used in the gas well deliquification (Osman, et al., 2010). Liquid loading problem arises once the velocity of produced gas drops lower than the critical velocity. The experimental results indicate that it is effective to evaporate the moderately saline water with microwave heating while it takes longer time for producing high salinity water.

2 Reservoir Model

In the reservoir heating simulation, the microwave device is lowered to the target formation and heats up the reservoir rock and interstitial fluids. The microwave device is operating at 2.45GHz and the power of 1000 Watt, which could be adjusted according to the heating

requirements, and the microwave is directed to the formation through a TE_{10} mode rectangular waveguide. Simulation has been conducted in ANSYS and CMG. The numerical simulation has been run following the flowchart indicated in Figure 3.

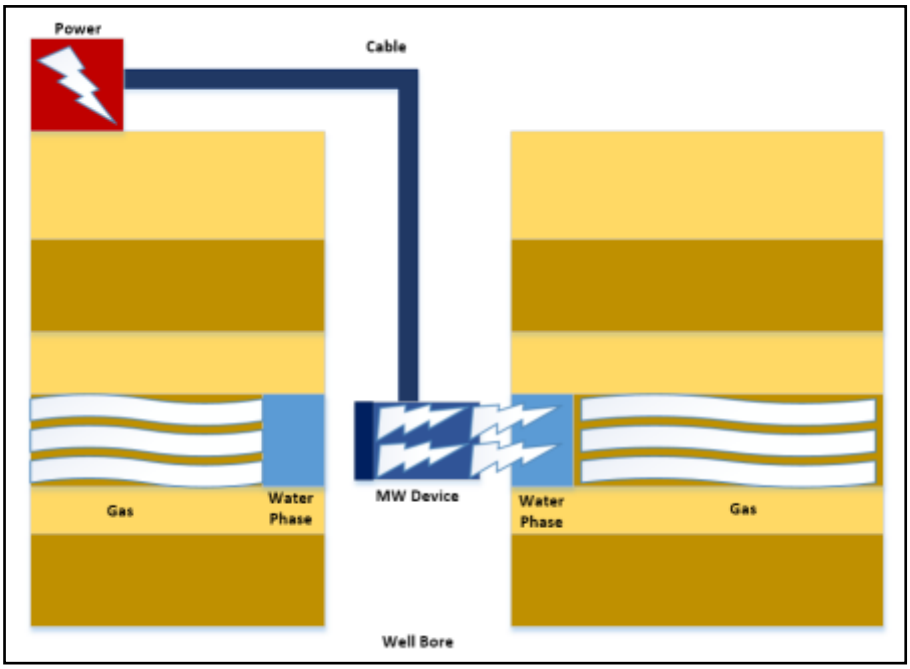

Figure 2 Concept Figure of Heating Formation with Microwave

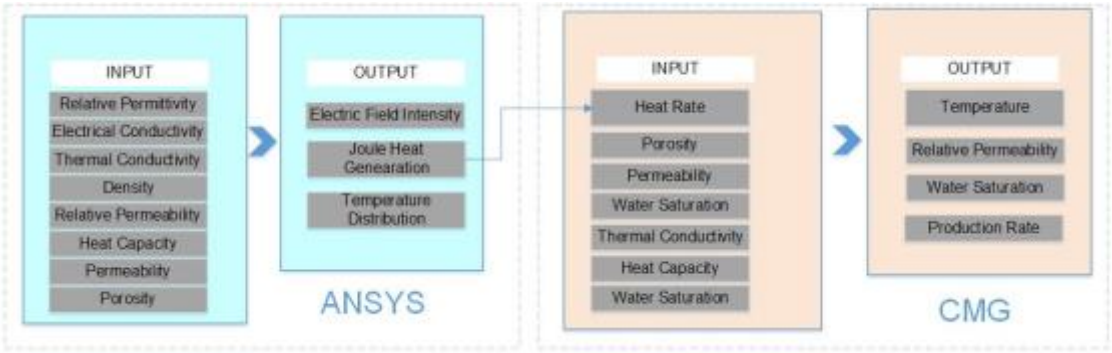

Figure 3 Flowchart Describing the Inputs and Outputs in ANSYS and CMG

The values of reservoir properties are listed in Table 2. After applying microwave to the reservoir, the electric field distribution and then the temperature in the reservoir can be computed in this model. The power dissipation rate is also one of the important outputs from the simulation and will be a critical input in the subsequent reservoir simulation.

Table 2 Reservoir Properties Used in the Simulation

Parameter	Value
Reservoir Temperature (°C)	139
Reservoir Porosity (1)	0.1
Reservoir Permeability (mD)	0.1
Initial Water Saturation (1)	0.3
Critical Water Saturation (1)	0.6
Reservoir Depth (m)	4000
Thermal Gradient (°C/100m)	2.8
Surface Temperature (°C)	27
Thermal Conductivity (J/ (m· day·°C))	1.73×10^{5}
Heat Capacity (J/ (cm^3 ·°C))	2.385
Microwave Frequency (MHz)	2450
Operation Power (Watt)	1000
Fracture Half Length (m)	100
Fracture Porosity	0.8
Fracture Permeability (mD)	3000

The numerical model was built in ANSYS with the geometry illustrated in Figure 4. The excitation method is rectangular waveguide (TE10) mode. The excited electromagnetic wave (2.45GHz) propagates through the reservoir sandstone and generated heat.

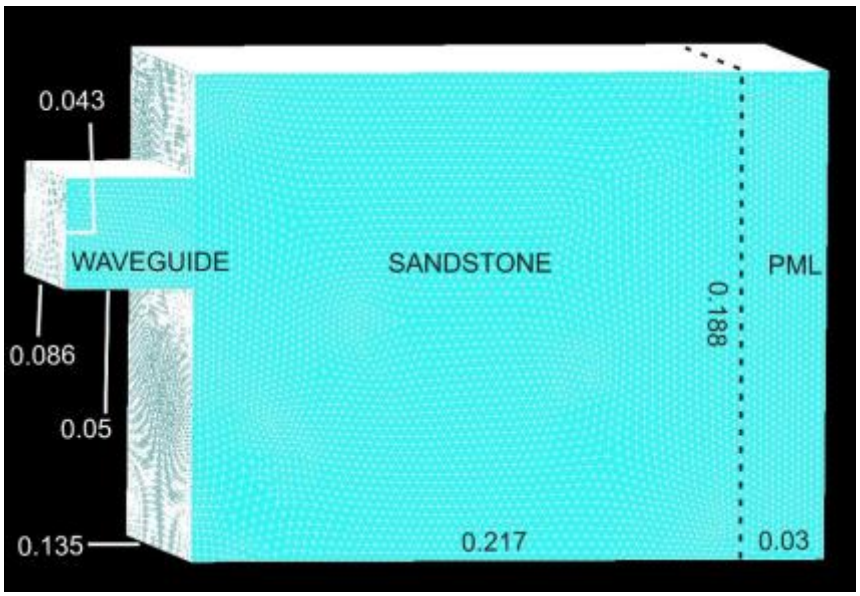

Figure 4 The Geometry Dimensions and Meshing of Numerical Model (Waveguide is the microwave device located in the wellbore and radiate microwave to the reservoir; sandstone is the object formation; PML is the layer absorbing microwave, so that the microwave will not be reflected by the boundary.

Different mesh sizes, namely no refinement mesh, minimum refinement, medium refinement and maximum refinement, have been applied to the model in order to investigate the grid dependency. As shown in grids, regardless of its level, the output is reliable.

Table 3, the large mesh sizes yield greater results, while three refinement sizes have smaller and similar results. So as long as the refinement has been conducted on the grids, regardless of its level, the output is reliable.

Table 3 Grid Dependency in ANSYS

	Maximum Electric Field (V/m)	Dielectric Power (Watt)	Maximum Joule Heat (Joule)	Maximum Temperature (°C)
No Refinement	32816	267	0.394×10^7	387
Minimum Refinement	30139	186	0.135×10^7	265
Medium Refinement	30164	183	0.165×10^7	264
Maximum Refinement	30135	184	0.206×10^7	268

The electric field distribution and Joule heat generated in the reservoir are shown in Figure 5. The maximum electric field strength is 30164 V/m. The average dissipated power is 183 Watt and daily Joule heat generation is around 2.87×10^9 Joule/m^3 in the near wellbore region. The reservoir simulation has been carried out in STARS-CMG and coupled with ANSYS Multiphysics.

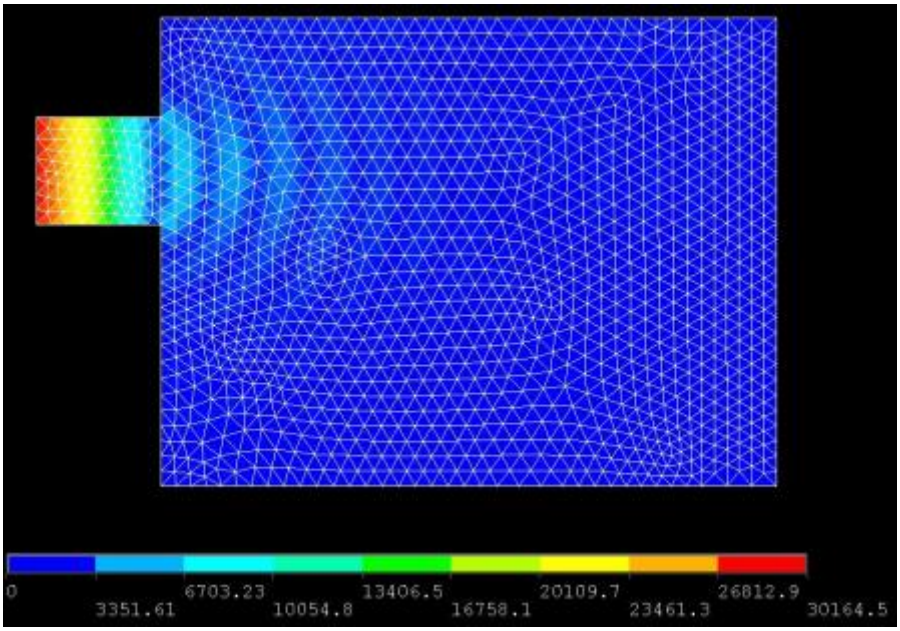

Figure 5 Electric Field Distribution (V/m) in the Reservoir (The maximum electric field is in the region near the source and its value is 30164 V/m. The microwave penetrates over 10 cm in the reservoir with electric field decreasing to around 6703.23 V/m).

3 Microwave Heating in Tight Gas Reservoir

The well was injected with water for 5 days to simulate the water invasion process and then the producer started to produce water and gas. Two scenarios considered in this paper are: the

well producing without microwave heater and with microwave heater. To simplify the problem, the reservoir properties were set to be temperature independent.

After the injector operated for 5 days, the water saturation in the near wellbore area increased from 0.3 to around 0.83 and the invasion depth reached as far as 1.16 m (Figure 6a). Then the gas well was put to production, but the water saturation near the wellbore remained at a higher value at around 0.7 (Figure 6b). Accordingly, the gas relative permeability decreased with the increase of water saturation to almost 0 after water injection (Figure 6c) and the formation damage persisted after water injection stopped (Figure 6d). To increase the relative permeability to gas, one method is to remove water phase trapped in the near wellbore area by applying intensive heat to target formation. The simulation used four downhole microwave devices, each with the same operation parameters as in FEM simulation abovementioned, to generate heat in four different directions in the wellbore. The reservoir size is 291m (length) ×291m (width) ×100m (thickness).

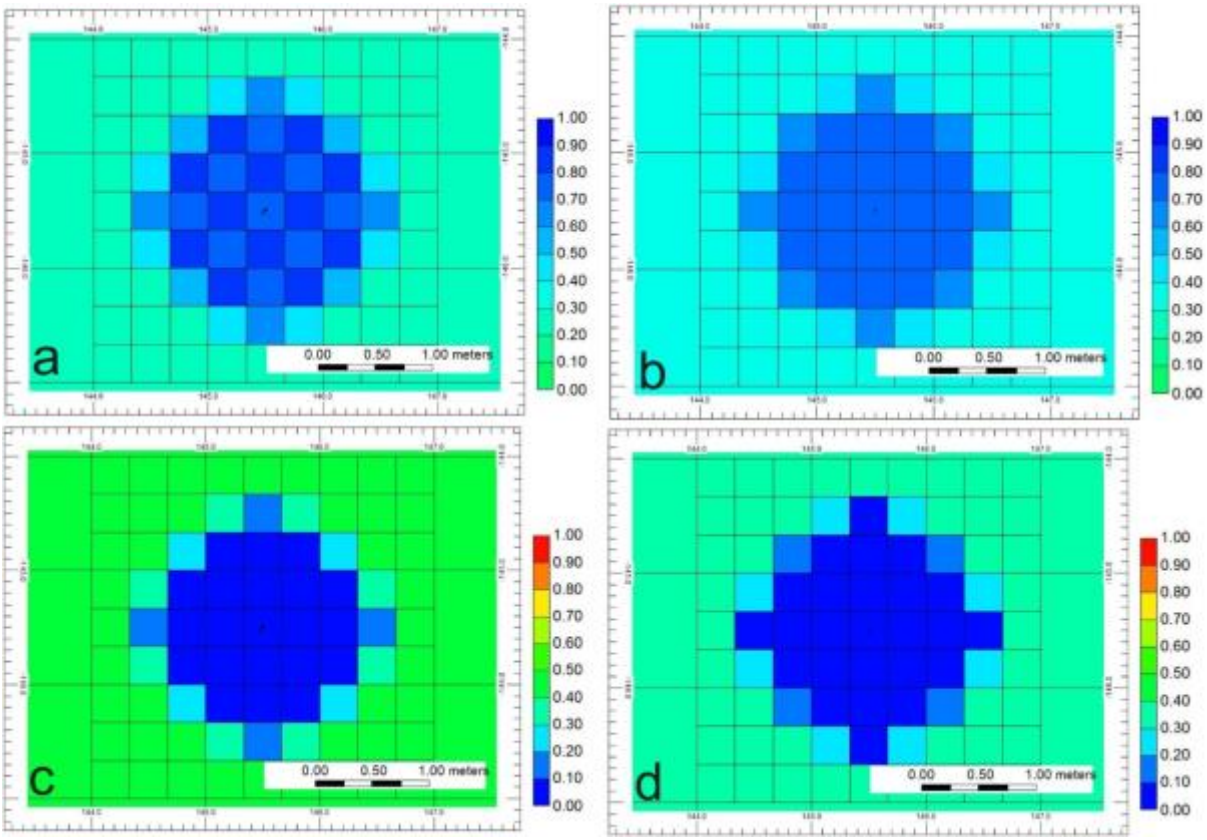

Figure 6 Water Saturation Distribution and Relative Permeability to Gas in the Well without Heater. (a indicates the water saturation distribution after injecting water for 5days; b is the water saturation distribution after 3-day production; c is the relative permeability to gas after injecting water for 5 days; d is the relative permeability to gas after producing for 3 days)

Coupled with ANSYS Multiphysics, with suitable input of reservoir properties, CMG computes the temperature distribution as well as water saturation and relative permeability to gas in the heated formation. The temperature of injected water is set the same as the reservoir temperature, so it does not affect the reservoir temperature (Figure 7a). During gas production, the microwave heater was switched on, thus the reservoir temperature increased up to 853 °C after 3-day heating (Figure 7b) and the heating depth of microwave is limited to approximately 83cm due to low thermal conductivity.

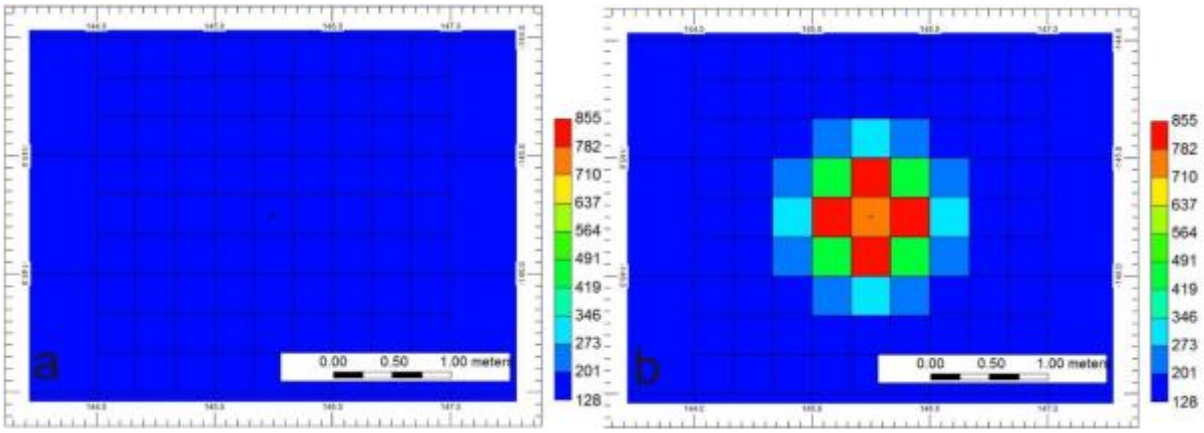

Figure 7 Temperature Distribution in the Formation at the End of Injection (a) and at the End of production (b) in the Well with Heater

As shown in Figure 8a and c, the water saturation increased from 0.3 to 0.8 and relative permeability to gas decreased to zero after water injection, which indicates a sever formation damage has happened. Consequently, the well failed to produce gas after water invasion and the pores are blocked by water around the well. During production period, the downhole microwave heater was employed to heat up the reservoir. The heat generation rate is 6.4×10^{8} Joule/day in one grid, which is within the penetration depth of microwave. The application of heat brought down the water saturation in the near wellbore area by evaporating water phase. In Figure 8-b, the water saturation dropped from 0.8 to 0 near the wellbore. Moreover, the relative permeability increased in the heated formation from almost 0 to almost 1 (Figure 8-d) because of the water phase has been removed by evaporation.

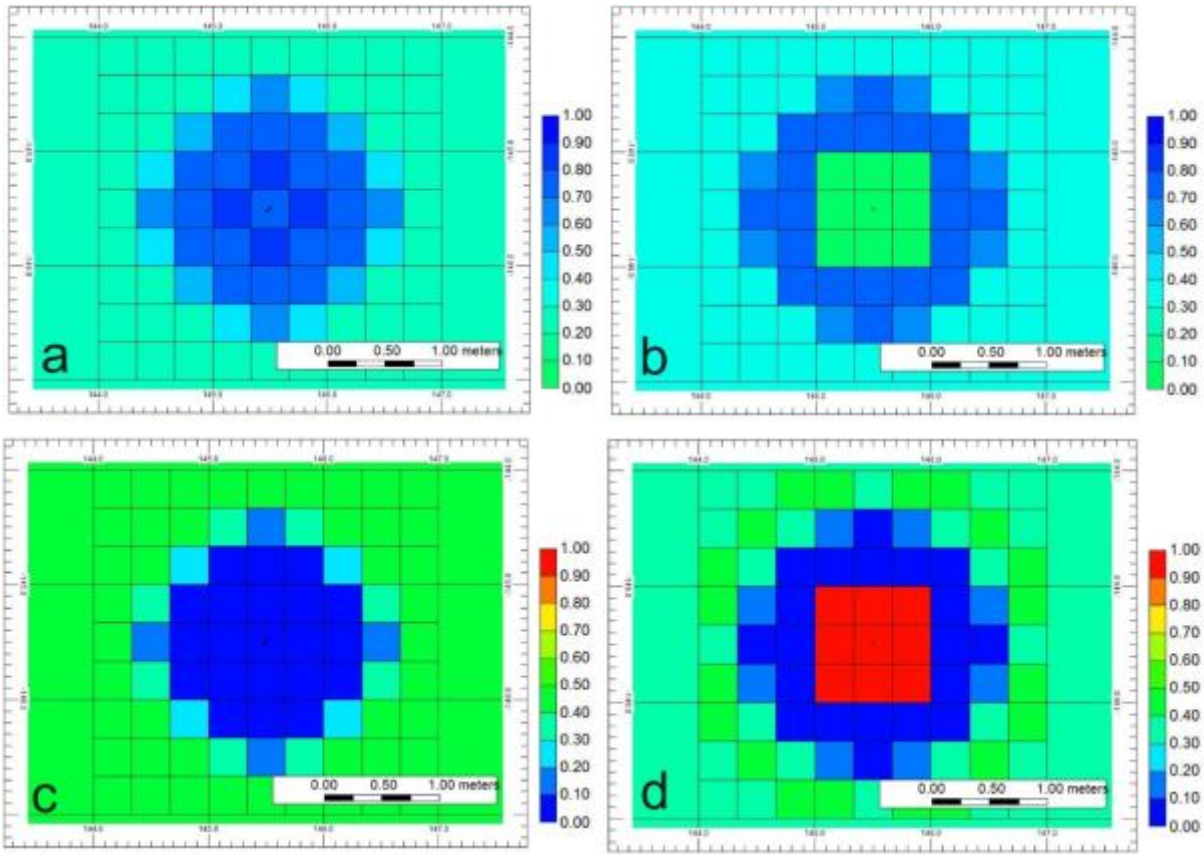

Figure 8 Water Saturation Distribution and Relative Permeability to Gas in the Well with Heater. (a is the water saturation distribution after injecting water for 5 days; b is the water saturation distribution after 3-day production; c is the relative permeability to gas after injecting water for 5 days; d is the relative permeability to gas after producing for 3 days)

The gas production rate and the cumulative gas production are compared for heated well and non-heated well. In Figure 9, the cumulative gas production is higher in the heated well than the non-heated well increasing from 4.0×10^6 m^3 to 4.4×10^6 m^3 in 90 days while the daily gas rate reached to $5.3\times10^4 m^3$/day compared with $3.8\times10^4 m^3$/day on the 15^{th} day. After that the performance of both wells is steady at $5\times10^4 m^3$ and $4.8\times10^4 m^3$ respectively. To some extent, the microwave heating is effective in improving the gas production rate.

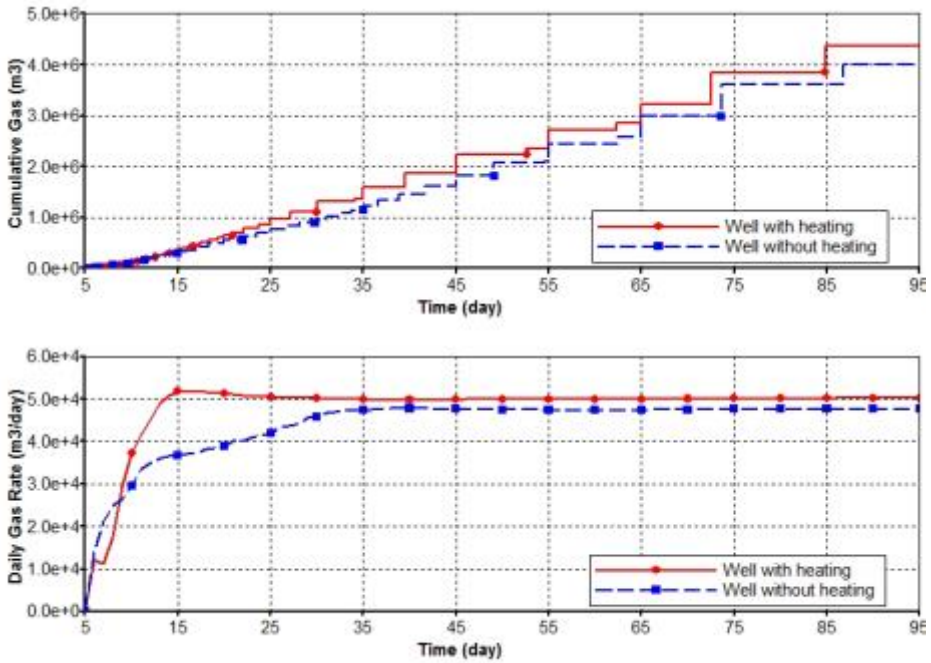

Figure 9 Gas Production Rate and Cumulative Gas Production in Tight Gas Well with MW Heating and without MW Heating.

To investigate the influence of grid size on the results, three models with different grid numbers have been built and run. The computed cumulative gas and daily gas rate have been compared in Figure 10, which shows a very close result for three grid sizes.

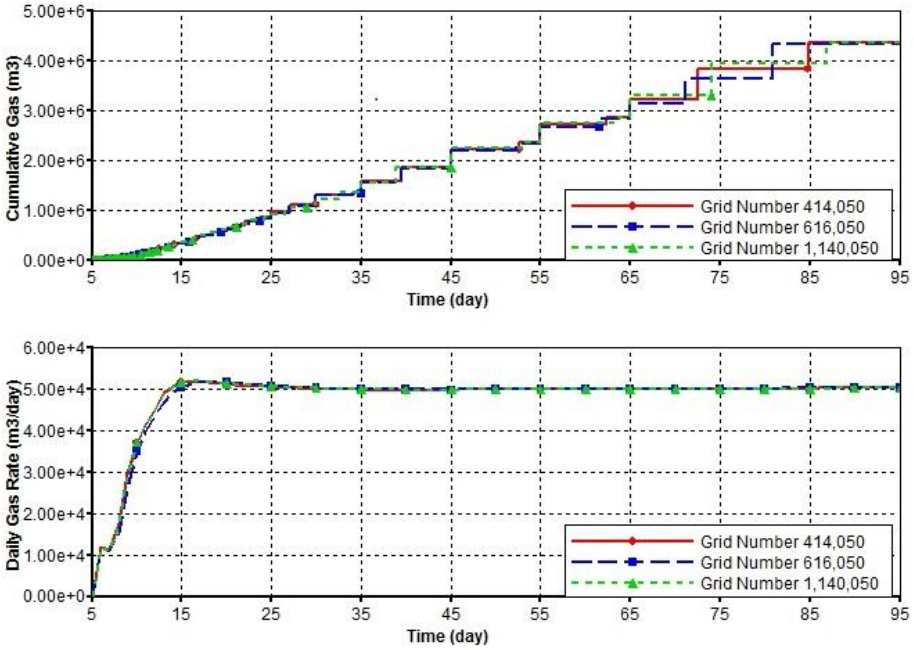

Figure 10 Grid Dependency Analysis in CMG-STARS

The sensitivity analysis has been conducted on the matrix permeability, thermal conductivity and heat capacity. The value of matrix permeability ranges from 0.1 to 50 mD, while that of

thermal conductivity and heat capacity ranges from $0.5\times10^5$to 2.5×10^5J/ (m· day·°C) and from 2 to 2.8 J/ (cm^3 ·°C) respectively. As shown in Figure 11, the heat capacity and thermal conductivity of sandstone have the minimal influences on cumulative gas production in the microwave-heated well. The less heat capacity, the greater cumulative gas production, and the less thermal conductivity the greater cumulative production. The matrix permeability has a greater influence on the gas production in the microwave-heated well. The microwave heating improved more gas production in the higher permeable reservoir.

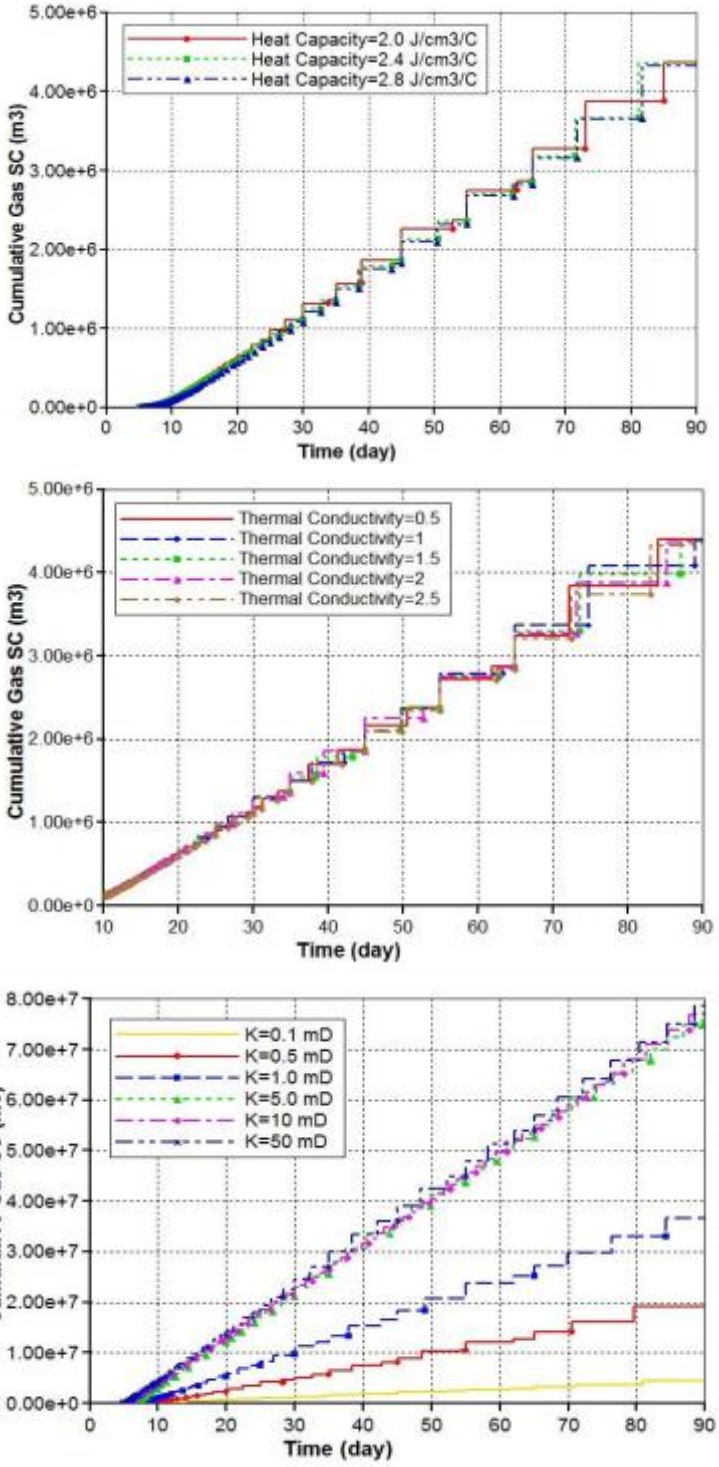

Figure 11 Sensitivity Analysis on Reservoir Rock Properties. The heat capacity values taken are 2, 2.4 and 2.8 J/(cm^3·°C), the thermal conductivities are 0.5, 1, 1.5, 2, and 2.5 ×10^{5}J/ (m· day·°C) and the permeability values are 0.1, 0.5, 1, 5, 10 and 50 mD.

4 Comparison of Simulation Solutions

The joule heat induced by microwave radiation in the reservoir is computed with ANSYS. With increasing penetration depth into the reservoir, the value of joule heat decreased (Figure

12). The maximum joule heat generation is 1.65×10^6 J/m^3, and the influenced depth reached about 10 cm.

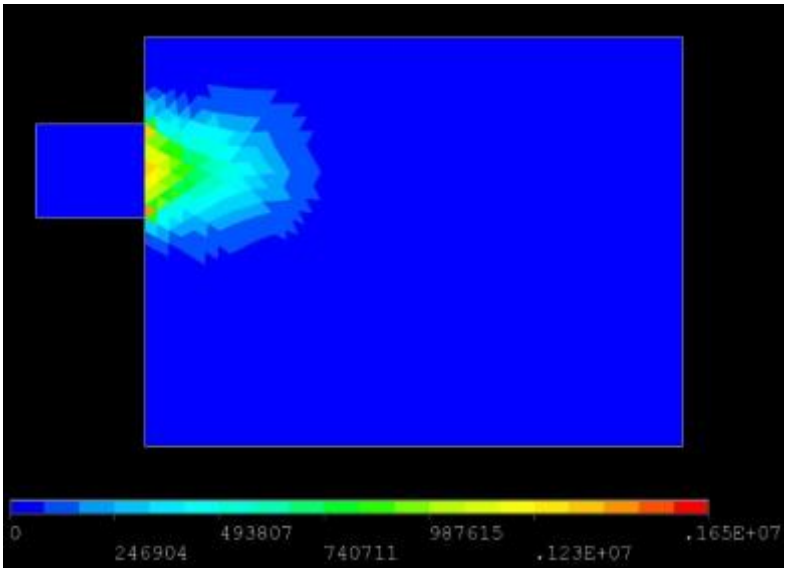

Figure 12 Joule Heat Distribution in the Reservoir.

The temperature distributions in the reservoir are computed in ANSYS software and CMG-STARS. Two results are compared with each other to verify the reservoir microwave heating method.

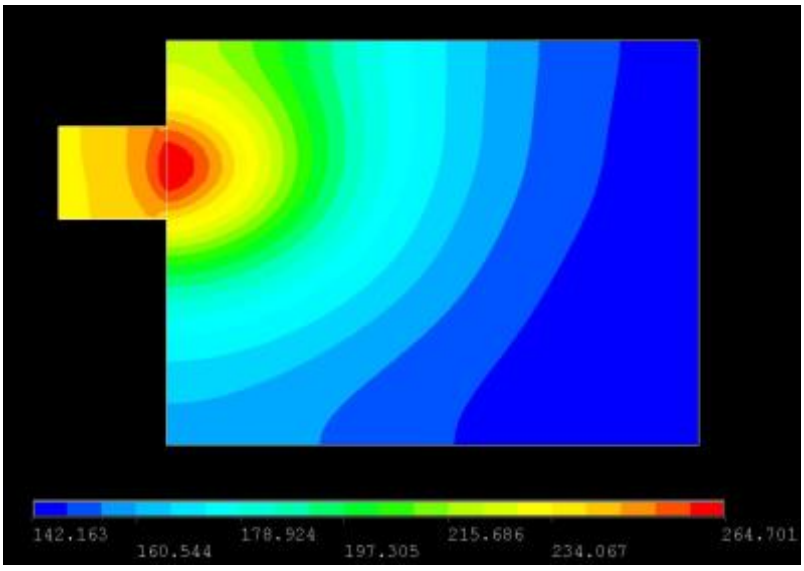

Figure 13 Temperature Distribution after Heating with Microwave for 30 minutes in ANSYS

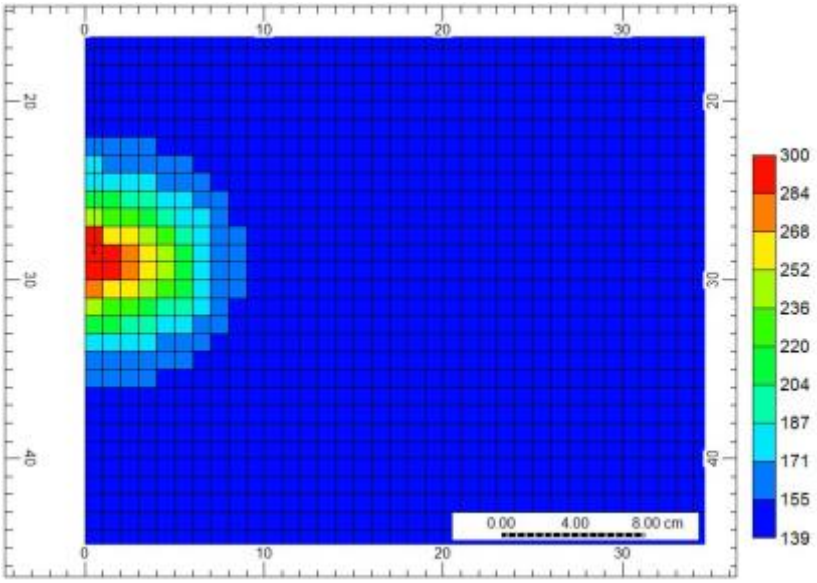

Figure 14 Temperature Distribution after Heating with Microwave for 30 minutes in CMG-STARS

According to Figure 13 and Figure 14, after 30-minute microwave heating, the highest temperature in the target formation reached over 300 °C in both computation methods. The influence depth of microwave heating reached about 10cm in 30 minutes. Comparison of solutions from CMG and ANSYS are plotted in Figure 15. The Finite Element Method (FEM) model shows a little bit lower temperature than CMG-STARS model near the wall of wellbore but the differences decreases with increasing distance to the wellbore. The temperature distributions with distance have a good correlation.

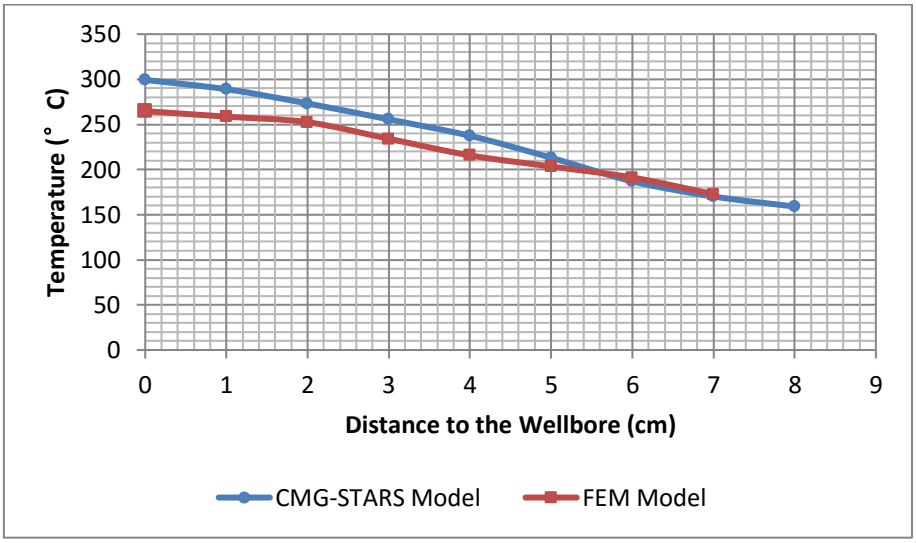

Figure 15 Temperature versus Depth in CMG Model and FEM Model

5 Microwave Heating in the Lab

To validate the FEM, a 2D Model has been constructed to simulate the heating of core plugs by microwave, and the results are compared with laboratory heating data. Details of the

simulation are described below. The microwave oven operates at 2.45GHz with power 1000 Watt. In this model, the dimension of waveguide used 109.22mm×50mm. The dimension of microwave oven plays a critical role in the distribution of electric field. For rectangular oven, one or more dimensions are several half wavelengths long at the excitation wavelength (Meredith, 1998). In this model, the wavelength is 122mm (half wavelength 61mm), so the oven internal dimension is 427mm×366mm.

5.1 Parameters of Sandstone Plug

Tight sandstone samples are collected from Perth Basin, Western Australia. The petrophysical properties are measured in the lab as the input properties of sandstone in the model (Table 4). The electrical properties, electrical conductivity and relative permittivity, of three samples are measured at 2.45GHz (Table 5).

Table 4 General Parameters for Simulation

Property	Value	Unit
Thermal Conductivity	2	W/(m*K)
Density	2650	Kg/m3
Relative Permeability	1	1
Heat Capacity	900	J/(kg*K)
Permeability	9.87e-17	m2
Porosity	0.1	1

Table 5 Electrical Properties at 2.45GHz of Tight Sandstone Samples

Property	Value	Unit
WR-1 Relative Permittivity	7.19-0.49i	1
WR-1 Electrical Conductivity	0.21	S/m
WR-11 Relative Permittivity	5.18-0.20i	1
WR-11 Electrical Conductivity	0.027	S/m
W-ERREG Relative Permittivity	6.93-0.665i	1
W-ERREG Electrical Conductivity	0.084	S/m

5.2 Temperature Distribution in Core Plugs

The electric field distributions are determined by the electrical properties of sandstone samples. Different relative permittivity and electrical conductivity are used for three tight sandstone plugs of WR-1, WR-11 and W-ERREG. More importantly, the different electric field distributions in the core plug lead to a different temperature distribution. In Figure 17, the differences of temperature distribution in the core plugs are distinct. Firstly, the maximum temperatures in the samples are different in WR-1 (508°C), WR-11 (389°C) and W-ERREG (436°C). Atomic Energy of Canada Limited Research Company and Voss Associates

Engineering Ltd. (1990) considered the reason for the cut-off temperature is the surface reflection limits the heating process. The dielectric constant is of great importance in this phenomenon. The fraction of reflected power is expressed by dielectric constant and loss tangent as:

$$\boldsymbol{R} = \frac{\mathbf{1} - \sqrt{\mathbf{2}\boldsymbol{\varepsilon}'[\mathbf{1} + \sqrt{\mathbf{1} + (\boldsymbol{tan\delta})^{\mathbf{2}}}]} + \boldsymbol{\varepsilon}'\sqrt{\mathbf{1} + (\boldsymbol{tan}\,\boldsymbol{\delta})^{\mathbf{2}}}}{\mathbf{1} + \sqrt{\mathbf{2}\boldsymbol{\varepsilon}'[\mathbf{1} + \sqrt{\mathbf{1} + (\boldsymbol{tan\delta})^{\mathbf{2}}}]} + \boldsymbol{\varepsilon}'\sqrt{\mathbf{1} + (\boldsymbol{tan}\,\boldsymbol{\delta})^{\mathbf{2}}}}$$

The fraction of absorbed power is estimated as (Bykov, et al., 2001):

$$\mathbf{1} - \mathbf{R} \approx \mathbf{2}\sqrt{\frac{\mathbf{2}}{\boldsymbol{\varepsilon}'\,\mathbf{tan}\,\boldsymbol{\delta}}}$$

The dielectric constant of minerals increases with temperature in the manner of Figure 16. This leads to the fraction of absorbed power reduced to 0 and the fraction of reflected power rose close to 1.

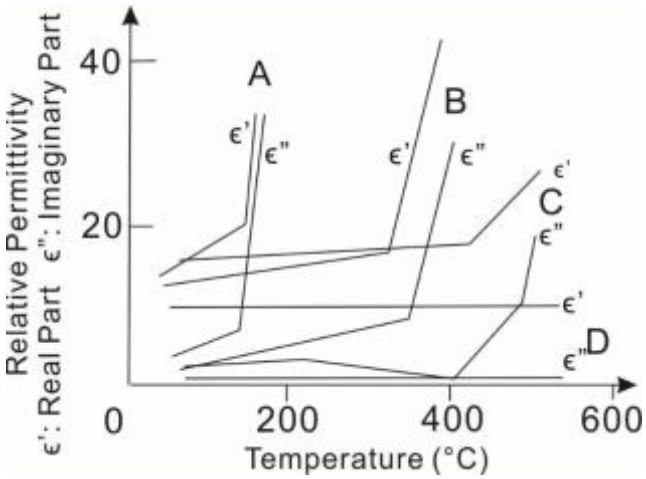

Figure 16 Dielectric Data for Four Sulphide Minerals and Ores at 2375MHz. (A: pyrrhotite, $Fe_{1-x}S$, where x lies between 0 and 0.2; B: chalcopyrite, $CuFeS_2$; C: pyrite, FeS_2 and D: sphalerite, ZnS. (After Atomic Energy of Canada Limited Research Company and Voss Associates Engineering Ltd., 1990.)

Secondly, the positions of the maximum temperatures in three samples vary with each other. The dielectric properties and electrical conductivity contribute to these differences by influencing the electric field distributions: the temperature is higher if the electric field is strong while the temperature is lower if the electric field is weak.

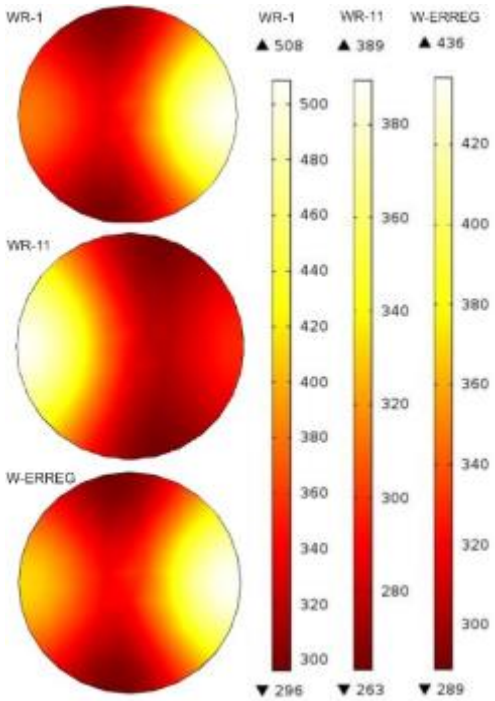

Figure 17 Numerical Modelling of Temperature Distributions for Three Tight Sandstone Samples in COMSOL.

5.3 Comparison of Surface Temperatures between Experiment and Numerical Modelling

The tight sandstone plugs are heated with microwave in the lab and surface temperatures are recorded with time. The simulated surface temperatures are plotted against time in the same coordinates. As indicated in Figure 18, the increase of surface temperature is nonlinear, both in simulation and in experiments, due to the complex mechanisms of microwave heating. The experimental data correlates well with the numerical modelling for the three tight sandstone samples WR-1, WR-11 and W-ERREG. The surface temperature reaches its maximum in 300s for WR-1 (500 °C), 480s for WR-11 (337 °C) and 360s for W-ERREG (409.8 °C).

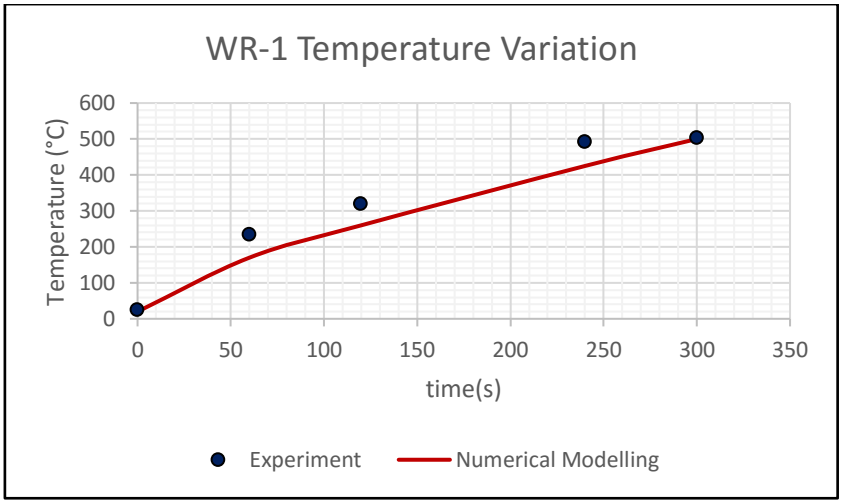

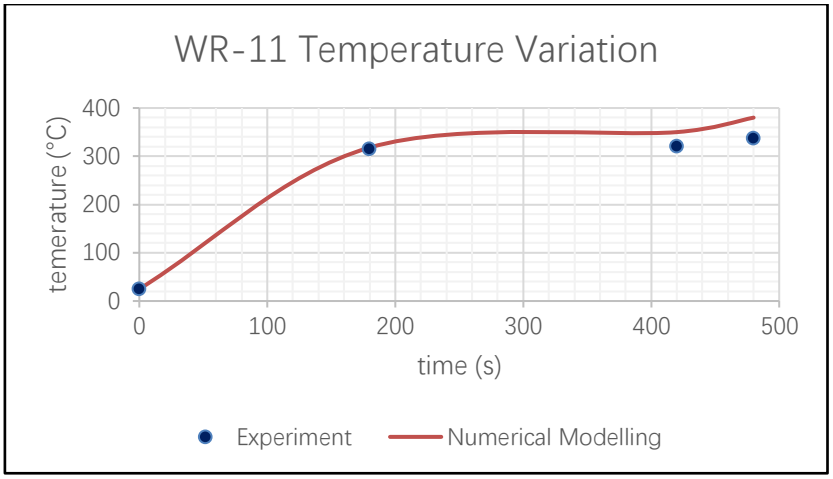

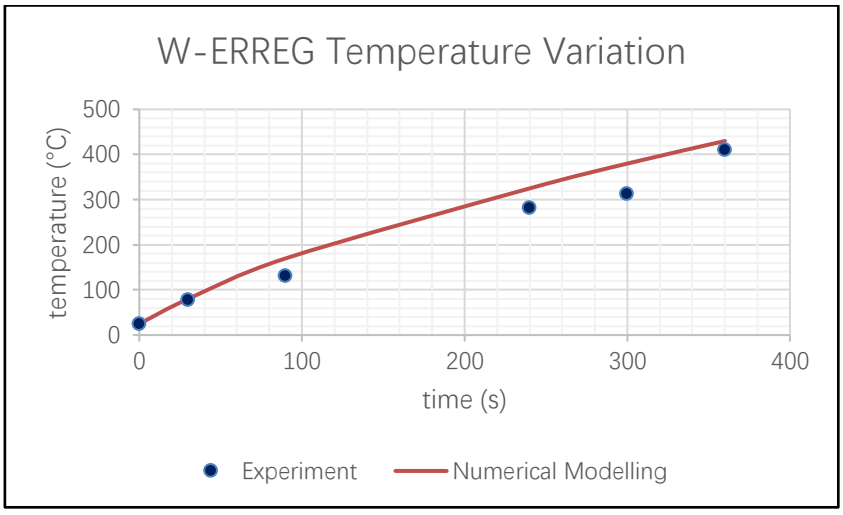

Figure 18 The Temperature Variations in Sample WR-1, WR-11 and W-ERREG.

6 Discussions and Conclusions

The Formation Heat Treatment with microwave has been simulated with FEM modelling software and reservoir modelling software. Two numerical modelling at the reservoir scale agree with each other well. Furthermore, the FEM simulation results are validated with laboratory data in the lab scale. The present study considered the effect of microwave heating on the formation only, the heating effects on fractures generation, clay shrinkage and chemical composition have not been considered. The absolute porosity and permeability may have a change due to heating. Furthermore, the temperature dependent reservoir properties need to be considered in the future to close the gap between numerical model and actual production. The penetration depth of electromagnetic wave is inversely proportional to its frequency. The microwave frequency used in this study is 2.45GHz. Alternatively, 915MHz microwave can be considered to increase the penetration depth of microwave. However, the design of the downhole needs to be modified accordingly.

Based on the above study, we come to the following conclusions:

1. The reservoir temperature reached up to 853 ℃ after 3-day production and heating, and due to the low thermal conductivity, the heating depth reaches about 83 cm. Nevertheless, the heating depth is sufficient for removing skin damage in the reservoir with porosity ranging from 8% to 20%.
2. The increase of water saturation in the near wellbore area causes the drop in relative permeability to gas and production. However, by elevating the reservoir temperature dramatically, the water saturation has been successfully brought down and the relative permeability to gas has been significantly improved.
3. The sensitivity analysis on reservoir properties revealed that, in the process of microwave heating treatment, the heat capacity and thermal conductivity have less influence on gas production improvement while the matrix permeability has a greater influence on it.
4. When the proper electrical conductivity and relative permittivity are provided, the FEM simulation agrees well with the experimental data in terms of the surface temperature of sandstone plugs.
5. Two simulation methods have a good correlation in computing the reservoir temperature. Moreover, the FEM simulation can be an effective method to predict the temperature distribution in an actual well.

Acknowledgement

Part of the content in the paper has been presented in the SPE Asia Pacific Unconventional Resources Conference and Exhibition, 9-11 November, Brisbane, Australia. The authors would like to thank the Unconventional Gas Research Group in Curtin University for providing support for the experimental work, and China Scholarship Council and China-Australia Gas Fund for providing financial assist. Finally, we want to express our appreciation to ANSYS, COMSOL and CMG for providing software licenses for this study.

References

Atomic Energy of Canada Limited Research Company and Voss Associates Engineering Ltd., 1990. Microwaves and Minerals. Energy, Mines and Resources Canada.

Bahrami, H., Rezaee, R. and Clennell, B., 2012. Water blocking damage in hydraulically fractured tight sand gas reservoirs: An example from Perth Basin, Western Australia. Journal of Petroleum Science and Engineering, 88, pp.100-106.

Bahrami, H., Rezaee, M.R., Ostojic, J., Nazhat, D.H. and Clennell, M.B., 2011, January. Evaluation of damage mechanisms and skin factor in tight gas reservoirs. In *SPE European Formation Damage Conference*. Society of Petroleum Engineers.

Bennion, D.B., 2002. An overview of formation damage mechanisms causing a reduction in the productivity and injectivity of oil and gas producing formations. *Journal of Canadian Petroleum Technology*, *41*(11).

Bennion, D.B., Thomas, F.B., Bietz, R.F. and Bennion, D.W., 1996. Water and hydrocarbon phase trapping in porous media-diagnosis, prevention and treatment. *Journal of Canadian Petroleum Technology*, *35*(10).

Binner, E., Lester, E., Kingman, S., Dodds, C., Robinson, J., Wu, T., ... & Mathews, J. P. (2014). A review of microwave coal processing. Journal of Microwave Power and Electromagnetic Energy, 48(1), 35-60.

Bykov, Y.V., Rybakov, K.I. and Semenov, V.E., 2001. High-temperature microwave processing of materials. *Journal of Physics D: Applied Physics*, *34*(13), p.R55.

Chen, J. H., Georgi, D., Liu, H. H., & Lai, B. (2015, August). Fracturing Tight Rocks by Elevated Pore-Water Pressure using Microwaving and its Applications. In SPWLA 56th Annual Logging Symposium. Society of Petrophysicists and Well-Log Analysts.

Computer Modelling Group LTD, 2015. STARS User Guide.

Kumar, H., Lester, E., Kingman, S., Bourne, R., Avila, C., Jones, A., ... & Mathews, J. P. (2011). Inducing fractures and increasing cleat apertures in a bituminous coal under isotropic stress via application of microwave energy. International Journal of Coal Geology, 88(1), 75-82.

Li, G., Meng, Y. and Tang, H., 2006, January. Clean up water blocking in gas reservoirs by microwave heating: laboratory studies. In *International Oil & Gas Conference and Exhibition in China*. Society of Petroleum Engineers.

Meredith, R.J., 1998. *Engineers' handbook of industrial microwave heating* (No. 25). IET.

Metaxas, A.A. and Meredith, R.J., 1983. *Industrial microwave heating* (No. 4). IET.

Miesch, E. P., & Albright, J. C. 1967. A Study of Invasion Diameter. In SPWLA 8th Annual Logging Symposium. Society of Petrophysicists and Well-Log Analysts.

Osman, M.K., Ghodke, N.T. and Al-Dogail, F.S., 2011, January. Gas Well Deliquificatin Using Microwave Heating. In *SPE Production and Operations Symposium*. Society of Petroleum Engineers.

Rider, M. H. 1986. The geological interpretation of well logs. Rider-French Consulting Ltd.

Thostenson, E.T. and Chou, T.W., 1999. Microwave processing: fundamentals and applications. *Composites Part A: Applied Science and Manufacturing*, *30*(9), pp.1055-1071.

Wang, H., Rezaee, R. and Saeedi, A., 2015, November. Evaluation of Microwave Heating on Fluid Invasion and Phase Trapping in Tight Gas Reservoirs. In *SPE Asia Pacific Unconventional Resources Conference and Exhibition*. Society of Petroleum Engineers.

Wang, H., Rezaee, R., & Saeedi, A. (2016). Preliminary study of improving reservoir quality of tight gas sands in the near wellbore region by microwave heating. Journal of Natural Gas Science and Engineering, 32, 395-406.

Yan, J., Jiang, G., & Wu, X. 1997. Evaluation of formation damage caused by drilling and completion fluids in horizontal wells. Journal of Canadian Petroleum Technology, 36(05).

Appendix A -The Conservation Equations in the CMG Numerical Model (Computer Modelling Group, 2015)

Two phases, water and gas, are considered in this paper. In order to discuss the conversation equations in this study, different terms are defined as below.

The accumulation term for water and gas: $\frac{\partial}{\partial t}[V_f(\rho_w S_w w_i + \rho_g S_g y_i)]$

The accumulation term for energy: $\frac{\partial}{\partial t}[V_f(\rho_w S_w U_w + \rho_g S_g U_g) + V_r U_r]$

The flow term of flowing component between two regions:

$\rho_w v_w w_i + \rho_g v_g y_i + \phi D_{wi} \rho_w \Delta w_i + \phi D_{gi} \rho_g \Delta y_i$

Where, the volumetric flow rates for water and gas $v_j = T(\frac{k_{rj}}{\mu_j r_j})\Delta\Phi_j$, j=w,g

The well source/sink term for flowing component: $\rho_w q_{wk} w_i + \rho_g q_{gk}$ $[well\ layer\ k]$

Where, $qjk = Ijk \cdot (pwfk - pk)$, j= w, g

The well source/sink term for energy: $\rho_w q_{wk} H_w + \rho_g q_{gk} H_g$

The flow term of energy between two regions:

$$\rho_w v_w H_i + \rho_g v_g H_g + \mathrm{K}\Delta\mathrm{T}$$

The heat loss source/sink term for energy:

$$\sum_{k=1}^{n_r} HL_k + HL_v + HL_c$$

The conservation equation for water and gas is:

$$\frac{\partial}{\partial t}[V_f(\rho_w S_w w_i + \rho_g S_g y_i)]$$

$$= \sum_{k=1}^{n_f}[T_w \rho_w w_i \Delta\Phi_w + T_g \rho_g y_i \Delta\Phi_g] + \sum_{k=i}^{n_f}[\phi D_{wi} \rho_w \Delta w_i + \phi D_{gi} \rho_g \Delta y_i]$$

$$+ \rho_w q_{wk} w_i + \rho_g q_{gk} y_i [well\ layer\ k]$$

The conservation equation of energy:

$$\frac{\partial}{\partial t}[V_f(\rho_w S_w U_g + \rho_g S_g U_g) + V_r U_r]$$

$$= \sum_{k=1}^{n_f} [T_w \rho_w H_w \Delta\Phi_w + T_g \rho_g H_g \Delta\Phi_g] + \sum_{k=1}^{n_f} K\Delta T + \rho_w q_{wk} H_w$$

$$+ \rho_g q_{gk} H_g[well\ layer\ k] + HL_o + HL_v + HL_c$$

Where,

Vf Volume of fluid phases added together

ρ density

S saturation

w_i water phase mole fraction

y_i gas phase mole fraction

U internal energies as a function of temperature and phase composition

V_r rock volume

U_r internal energies per rock volume

T the transmissibility between two regions

$\Delta\Phi_j$ the potential differences

I_{jk} phase j index for layer k

p_{wfk} flowing wellbore pressure in well layer k

p_k the node pressure of the region with well layer k

H the enthalpy

K thermal transmissibility at the interface between the two regions

ΔT the drop of temperature between the nodes

HL_k the rate of heat transfer to the region of interest through block face number k from the adjacent formation

Hl_v the rate of heat transfer from a convective model

HL_c represents a constant heat transfer model